ELSEVIER

Journal of Nuclear Materials 253 (1998) 36–46

journal of nuclear materials

Irradiation-enhanced creep in SiC: data summary and planned experiments

C.A. Lewinsohn [a,*], M.L. Hamilton [a], G.E. Youngblood [a], R.H. Jones [a], F.A. Garner [a], S.L. Hecht [b], A. Kohyama [c]

[a] *Pacific Northwest National Laboratory [1], Richland, WA, USA*
[b] *DE&S Hanford, Richland, WA, USA*
[c] *Kyoto University, Kyoto, Japan*

Abstract

Silicon carbide composites are under consideration for structural applications in proposed magnetic fusion energy systems. The limited data available suggest that creep of silicon carbide, like that of metals, is enhanced in a neutron environment. Existing irradiation-creep data on silicon carbide are reviewed and the ramifications of these data are discussed. Two experimental approaches to determine the irradiation creep of a silicon carbide composite are described. One of these utilizes a flat, reduced gage section specimen loaded in tension and the other utilizes a pressurized cylinder. © 1998 Elsevier Science B.V.

1. Introduction

One of the most promising candidate materials for use in magnetic fusion energy systems is a ceramic composite consisting of silicon carbide fibers (SiC_f) embedded in a silicon carbide matrix (SiC_m) [1–6]. This silicon carbide composite (SiC_f/SiC_m) could be used to construct the fusion system first wall and for construction of other important near-plasma components. The radioactivation of this composite material would be very low and in fact would be dominated by the activation of impurity elements [1–3]. Fabrication of these materials via chemical vapor deposition (CVD) of high-purity reactant gases would minimize the impurity content.

Irradiation creep is one of the major processes by which the dimensional stability of structural components can be altered by radiation exposure. There is only a small amount of data [7–9] on irradiation creep of silicon carbide (SiC) and no data on irradiation creep of SiC_f/SiC_m composite materials. To date the only relevant creep data have been generated very recently on SiC fibers using charged particle irradiation [9]. These limited data suggest that irradiation enhances creep in silicon carbide and, hence, the irradiation creep response of SiC_f/SiC_m composites should be investigated. This report will review the available irradiation creep data from SiC and describe a proposed approach to obtain irradiation creep data for SiC_f/SiC_m.

2. Review of silicon carbide irradiation creep data

The thermal creep behavior of silicon carbide has been studied carefully by Davis et al. [10–12], and other investigators [13–16]. Generally, for the fine grained microstructures of SiC_f/SiC_m composites, grain boundary-diffusion controlled creep will dominate dislocation or lattice-diffusion controlled creep. In addition, thermal creep in CVD silicon carbide, with a highly textured microstructure, is very anisotropic. In a study of the compressive creep behavior of CVD silicon carbide [11] deformation could not be measured, even under high stress, if the applied stress was parallel to the ⟨111⟩ direction of the grains.

* Corresponding author. Tel.: +1-509 372 0268; fax: +1-509 376 0418; e-mail: ca_lewinsohn@pnl.gov.

[1] Operated for the US DOE by Battelle Memorial Institute under Contract DE-AC06-76RLO 1830.

PII S0022-3115(97)00303-6

Initial studies of the irradiation creep behavior of silicon carbide were conducted by Price at General Atomics [7]. In these experiments, oriented graphite substrates were coated with pyrolytic β-silicon carbide and then irradiated in the ETR reactor (INEL) at 640 and 900°C at exposures of 3.2×10^{21} and 3.8×10^{21} nvt ($E > 0.18$ MeV), respectively. Irradiation-induced swelling of the graphite substrate put the silicon carbide in tension causing residual curvature from which the contribution due to irradiation creep could be deduced. These experiments provided rough estimates of the upper bounds of the steady state creep rate. The steady state creep rate, $d\varepsilon_c/dt$, was assumed to be linearly proportional to the product of stress, σ, and flux, ϕ

$$d\varepsilon_c/dt = K\sigma\phi. \quad (1)$$

The creep constant, K, was estimated to be on the order of 2×10^{-37} (Pa n/m^2)$^{-1}$ at 640°C. At 900°C an upper limit of 4×10^{-37} (Pa n/m^2)$^{-1}$ was inferred. These calculations did not account for plastic strain or chemical interaction between the silicon carbide and graphite.

In a later series of experiments [8], Price loaded thin strips of pyrolytic β-silicon carbide under constant strain in four-point flexural loading fixtures and subjected them to irradiation at 780, 950 and 1130°C in the ETR reactor (INEL). In addition, the specimens were fabricated at different temperatures to obtain grain sizes of 1, 5 and 10 μm. After irradiation the specimens were removed from the fixtures and the residual curvature was measured to obtain the amount of stress relaxation caused by creep. The insensitivity of the strain relaxation to the initial elastic strain confirmed that the creep rate was linearly proportional to stress.

The steady state irradiation creep constant, K, as a function of irradiation temperature, is shown in Fig. 1, as measured with the relaxation experiments [8]. For some

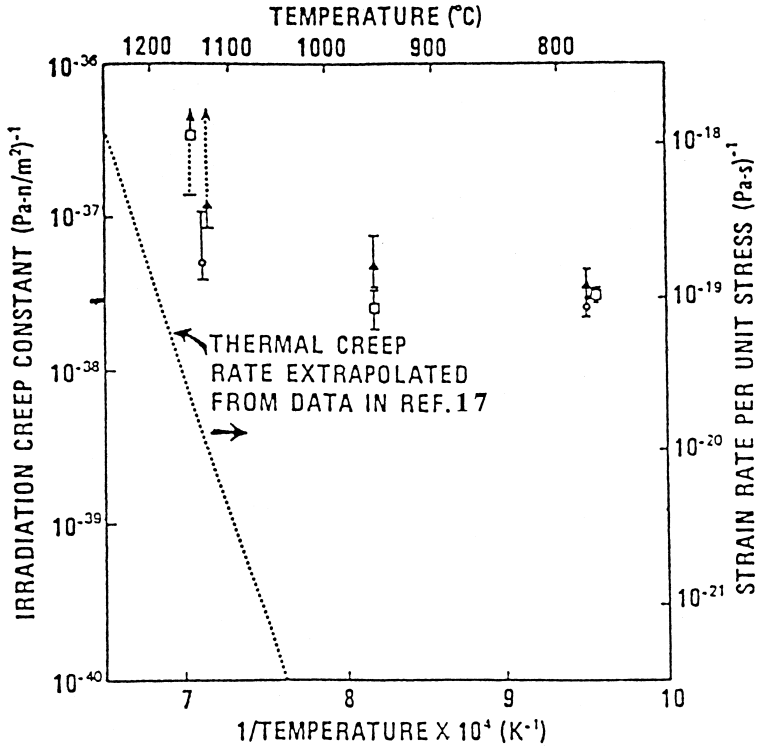

SYMBOL	DEPOSITION TEMP (K)	APPROX GRAIN SIZE (μm)
○	1673	1
▲	2023	5
□	2073	10

Fig. 1. Irradiation creep constant and strain rate as a function of temperature for pyrolitic SiC [8].

specimens at the higher temperatures, relaxation was almost complete and only a lower limit for the creep constant could be estimated. The axis on the right of the plot indicates the approximate steady-state creep rate per unit stress, and the dashed line indicates the calculated thermal creep rate [17]. The irradiation creep data shown in Fig. 1 are subject to substantial errors because of uncertainty and fluctuations in the temperature of 100 to 150°C and the neglect of transient creep in the analysis. At temperatures between 950 and 780°C the irradiation creep constant is relatively temperature independent.

Recently, the torsional creep response of silicon carbide monofilaments under charged-particle irradiation has been measured [9]. These fibers consist of grains of the cubic, 3C, polytype of silicon carbide deposited, via CVD, onto a 33 μm pitch-based carbon core. The cross section consists of seven distinct layers including a silicon containing carbonaceous outer coating, four regions of silicon carbide with varying carbon content and grain size, an inner layer of pyrolytic carbon and the carbon core [18,19]. Since the silicon carbide is produced by CVD, however, the grain structure and orientation is similar to the matrix of CVI SiC_f/SiC_m and, hence, is a good model material. The overall fiber diameter is approximately 140 μm. Under conditions of thermal creep, these fibers exhibit only primary creep behavior [20]. The results of the torsional irradiation experiments, shown in Fig. 2, indicate that creep of these fibers is greatly enhanced by irradiation. Quantitative measurements from these experiments have yet to be published. Analysis of the experimental results are complicated by the stress state on the fiber (shear stress in the outer layers), the response of the low-modulus carbon core, load-sharing effects among the distinct layers of the fiber, and equipment compliance calibrations. Nevertheless, the data shown in Fig. 2 indicate that the creep behavior of these fibers is enhanced by irradiation.

In summary, the data available for the irradiation creep of silicon carbide indicate that under certain conditions the creep rate of silicon carbide can be enhanced by 2–3 orders of magnitude, relative to thermal creep. In addition, there is some indication that below a certain temperature the steady state irradiation creep rate constant may be independent of temperature.

3. Proposed techniques for obtaining SiC_f/SiC_m composite irradiation creep

Two methods for obtaining the irradiation creep response of SiC_f/SiC_m will be described. The pressurized bladder approach is a modified technique based on a method used to study metals. The pressurized bladder approach is suited to small reactor spaces and is not specific to any particular reactor. The in-pile tensile specimen approach allows real time in-situ measurements to be made using established experimental apparatus and techniques. The results of a detailed analysis of the pressurized bladder approach will be summarized here. A similar analysis of the in-pile tensile specimen approach is currently underway.

Other approaches to measuring the irradiation creep of SiC_f/SiC_m have been proposed. These designs will not be discussed here, but each approach has specific advantages and disadvantages. To the best of the authors' knowledge, other techniques have not been analyzed to the extent of

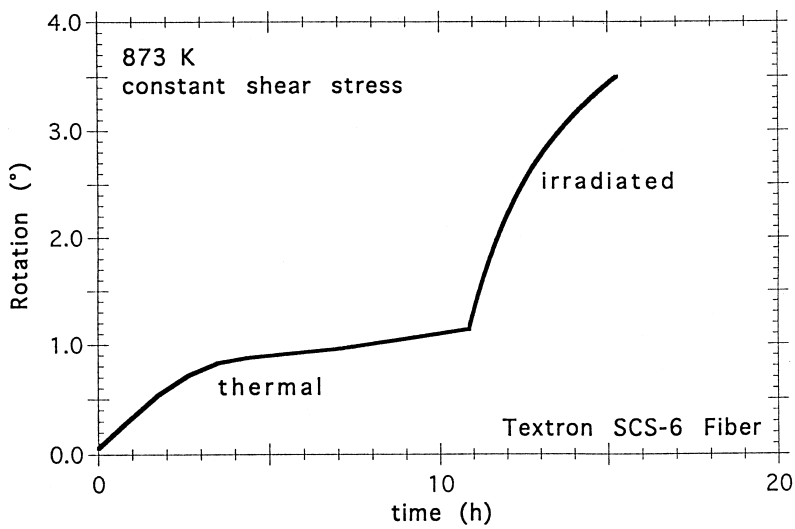

Fig. 2. Effect of charged particle irradiation on torsional deformation of silicon carbide monofilaments (after Ref. [9]).

the pressurized bladder, and hence their success remains uncertain. In addition, the present authors considered several other designs that were found to be less suitable, for a variety of reasons, than the pressurized bladder approach. Although other effects, such as irradiation-induced dimensional change and matrix cracking, may interfere with the intended creep strain measurements, the results of the experiment will be important in determining the response of SiC_f/SiC_m composites to stress while under irradiation and to identify critical issues in the radiation-stability of SiC_f/SiC_m composites. As discussed, the data currently available regarding irradiation creep of silicon carbide are not sufficient to determine whether it will occur in SiC_f/SiC_m composites in fusion energy systems. The experiment described in this paper will indicate whether irradiation-enhanced creep is more or less severe than irradiation-induced swelling or matrix cracking effects. If large amounts of irradiation creep occur, the experiment provides a means to obtain quantitative measurements.

3.1. The pressurized bladder irradiation creep experiment

The goal of this experiment is to obtain irradiation creep data which is representative of the design needs for a fusion energy system. The design conditions are specimen irradiation doses of 5–10 dpa and irradiation temperatures of 500–1000°C. Optimal stresses for studying mechanistic effects were chosen. Specimens will be investigated at stresses below, near and above the assumed matrix cracking stress. Although the experiment can be adapted to any available reactor space, the details described in this report are specific to the large removable beryllium (RB^*) mid-core location of the high flux isotope reactor (HFIR). The HFIR is assumed to operate at 100 MW power, and the experiment is expected to remain in the reactor for approximately 1 yr (300 effective full power days).

The pressurized bladder specimen consists of a SiC_f/SiC_m cylinder over a closed-end bladder of niobium–1 wt% zirconium pressurized with helium gas (Fig. 3). Helium was selected for maximum heat transfer and temperature uniformity. The pressure of the helium is chosen so that at the temperature of the specimen in the reactor thermal expansion of the gas provides the desired pressure. The specimen and bladder are designed to provide constant radial loading on the SiC_f/SiC_m cylinder which gives rise to a constant hoop stress. As discussed later, the surface of the bladder in contact with the specimen may be coated with an approximately 1 μm thick layer of alumina (Al_2O_3) to minimize adverse chemical interactions. Niobium–1 wt% zirconium was selected as the bladder material because of its combination of high-temperature strength and ductility, the ability to fabricate the desired components easily and it is the only refractory material for which irradiation creep data exist at the temperatures relevant to this experiment. The specimen and bladder are axially constrained by an additional niobium–1 wt% zirconium sub-assembly. The sub-assembly holds three SiC_f/SiC_m specimens, as well as four bar shaped specimens and seven holders for dimensional stability tests of ceramic fibers (Fig. 4).

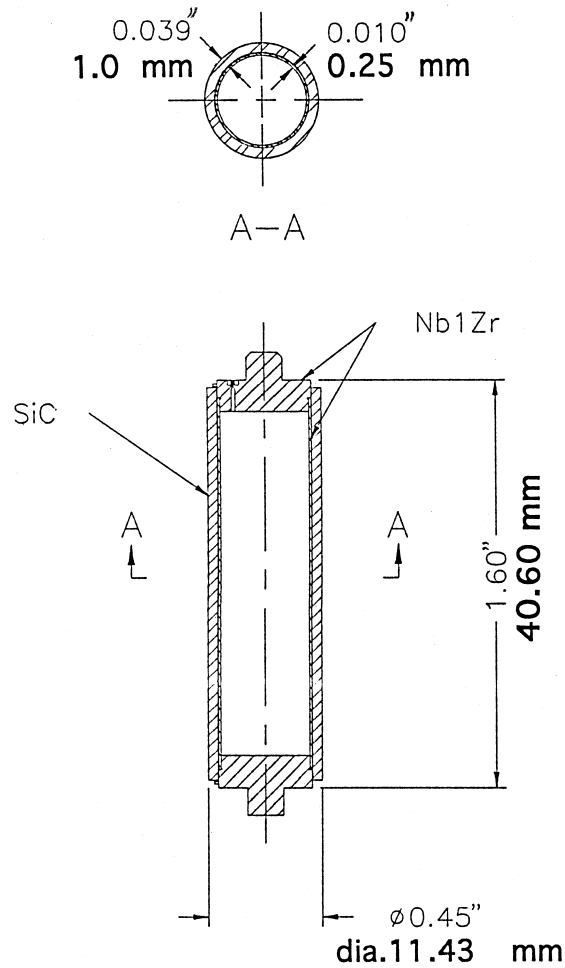

Fig. 3. Schematic drawing of the SiC_f/SiC_m composite tube specimen and niobium–1 wt% zirconium pressurized bladder.

Since the creep compliance of the bladder is several orders of magnitude lower than the SiC_f/SiC_m specimen, the tube deforms with the specimen and allows a constant pressure to be transmitted to the composite cylinder. The sub-assembly provides axial restraint to mitigate stress rupture due to axial creep. The temperature can be controlled during the experiment by adjusting the composition of the helium and neon gas mixture in the annular gap between the sub-assembly and the reactor capsule holder (RB^* subcapsule). After the experiment the change in the specimen dimensions will be measured using laser extensometry (resolution 0.5 μm) and the strains calculated accordingly.

Since irradiation-induced swelling of the SiC_f/SiC_m composites may interfere with measurement of the creep

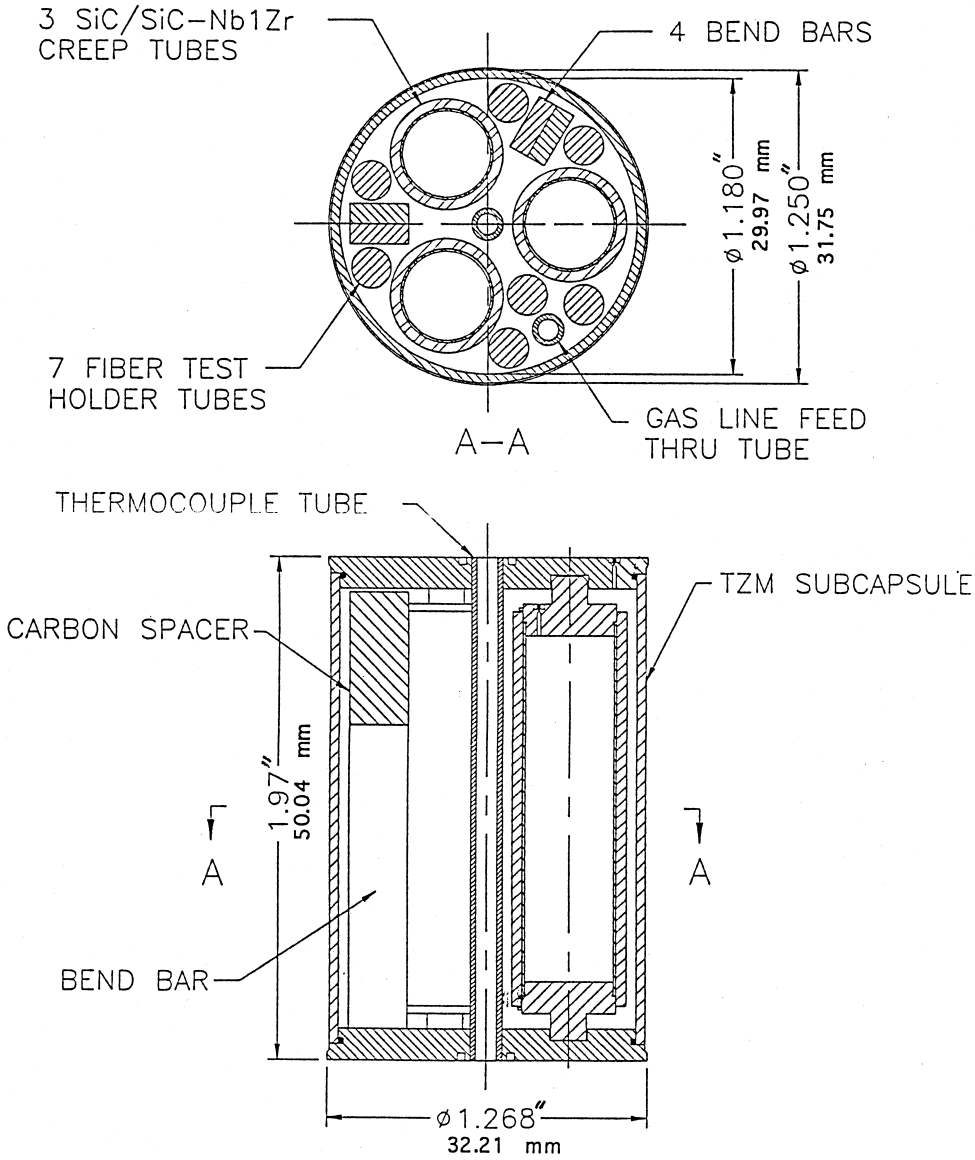

Fig. 4. Schematic drawing of the subassembly and specimens.

strain, separate SiC_f/SiC_m composite tubes without pressurized bladders will also be irradiated. Immersion density measurements and laser extensometer measurements of the tube dimensions, both before and after irradiation, will be used to determine the magnitude of the irradiation swelling. Additionally, thermal exposure of SiC_f/SiC_m composites and niobium–1 wt% zirconium bladders with and without composite specimens will be performed at the same temperature as the irradiated specimens, for the same length of time as the irradiation treatments, to determine the thermal creep component of the measured strain in the irradiated specimens. This approach is designed to determine if irradiation enhanced creep of SiC_f/SiC_m composites is a major concern in the use of these materials in radiation environments.

3.1.1. Stress analysis

A finite element model consisting of the pressurized niobium–1 wt% zirconium bladder and the SiC_f/SiC_m specimen tube was used to predict the stresses in the bladder and the specimen. The model considered internal gas pressure loading on the bladder tube, thermal expansion of both tubes, irradiation creep of both tubes and irradiation swelling of the niobium–1 wt% zirconium tube.

The ANSYS™ finite element analysis program was used for the two-dimensional (2D) axisymmetric (R-Z) model using axisymmetric shell elements (SHELL51) for the tubes and gap elements (CONTAC12) for the frictionless interaction mechanics. The finite element model (FEM) only considers radial deformations, as axial friction between the bladder and the specimen is assumed to be nonexistent. Neutron fluxes were assume to be those for the HFIR reactor RB* location. Analyses were performed for the two temperatures of interest, 800 and 1000°C.

Analysis of the experiment design at 800 and 1000°C, in which there was assumed to be a small initial room temperature diametrical gap of 2×10^{-5} m, indicated that a small permanent increase in diameter of approximately 4.6 μm (a measurable value) would be produced at the end of 300 effective full power days. The value of the expected diameter change is close to the practical limit of the laser extensometer system (≈ 5 μm) when inhomogeneity in the bladder surface is considered. Therefore, if the measured diameter change is below 5 μm it will be known that irradiation creep occurs at a rate below that used in the FEM model and may not be a lifetime limiting mechanism in fusion energy systems. On the other hand, larger measured changes in the diameter will allow quantitative evaluation of the composite creep rate. The deformation for both temperatures is comparable as the hoop stresses are equal and the creep rate is temperature independent below 1000°C. Fig. 5 shows the calculated hoop stresses in both the SiC_f/SiC_m specimen and the bladder tube during the irradiation, for both temperature conditions analyzed. The hoop stress in the specimen remains nearly constant over the life of the experiment.

3.1.2. Thermal analysis

Two 2D finite element thermal analyses, an R–Z axisymmetric analysis and a 2D sector analysis, were made to determine the temperature distribution of the test assembly. Both models use the ANSYS™ finite element analysis program. These analyses considered internal heat generation due to gamma heating, conduction/convection within the specimen/bladder and capsule, thermal radiation across gas gaps and convection to the reactor coolant.

The resulting temperature profile from the R–Z model for the 1000°C case is shown in Fig. 6. The maximum temperature in the HFIR RB* subcapsule is less than 200°C. The temperature drop across the control gas gap is approximately 650°C. The RB* subcapsule wall is at temperatures in the range of 870 to 890°C. An average 80°C temperature gradient is calculated within the RB* subcapsule, with a maximum average temperature of 950°C. The SiC_f/SiC_m specimen is expected to be at an average 1000°C. Similar results trends were predicted for the 800°C design.

The second thermal FEM, a 2D sector analysis, calculates in more detail the temperatures within the RB* subcapsule. This model (Fig. 7) is a 2D, 60° sector model (minimum section of symmetry) representing a slice through the axial center of the experiment. The model

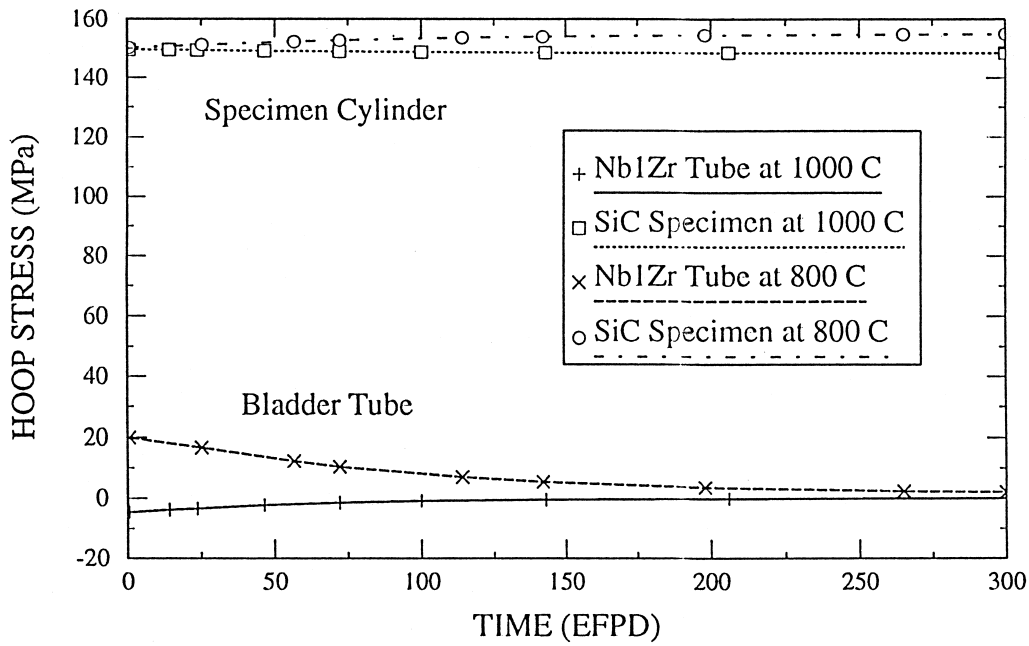

Fig. 5. Results of FEM stress analysis.

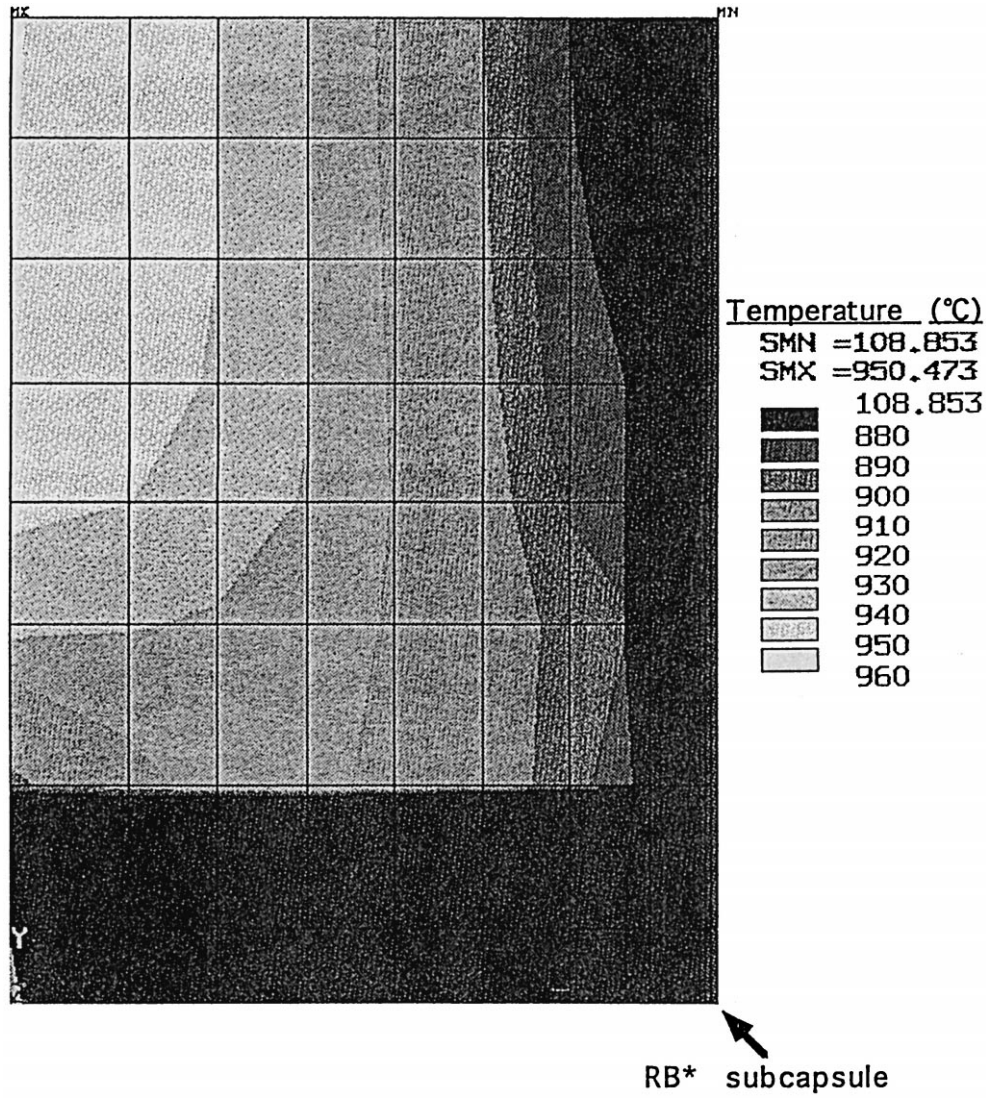

Fig. 6. Results of FEM R–Z temperature profile analysis.

comprises ANSYS 2D plane thermal conduction (PLANE55) elements and radiation link (LINK31) elements. Regions from the thermocouple tube to the reactor coolant were modeled. As this model does not consider heat flow in the axial direction, and is based on the tube-to-tube gaps, the predicted temperatures are expected to be higher than actual.

The overall temperature profile predicted by the 2D sector model is shown in Fig. 8. The temperature of the RB* subcapsule wall is about 170°C cooler than that predicted in the R–Z analysis and the gradient across the RB* capsule is 490°C, considerably more (as expected) than that predicted for the case with homogenized properties. When comparing the two cases, it is apparent that the sector model, which neglects the axial heat transfer effects, will overstate temperature gradients (axial effects and the thick end caps should mitigate the large temperature gradient). It is likely that the RB* wall will be hotter and that the specimen will be cooler than that shown in Fig. 8.

Several conclusions can be drawn from the results shown in Figs. 6 and 8. Firstly, the thermocouple measurement may be as much as 80°C higher than the average cylinder specimen temperature. Secondly, the temperature gradient around the circumference of the cylinder specimen may be as high as 150°C. Additionally, the average temperature in the passive SiC specimens may be as much as 100°C cooler than the cylinder specimen. Finally, the temperature gradients across the bend bar and fiber test holder specimens may be up to 130 and 90°C, respectively. Although the temperature gradient around the circumfer-

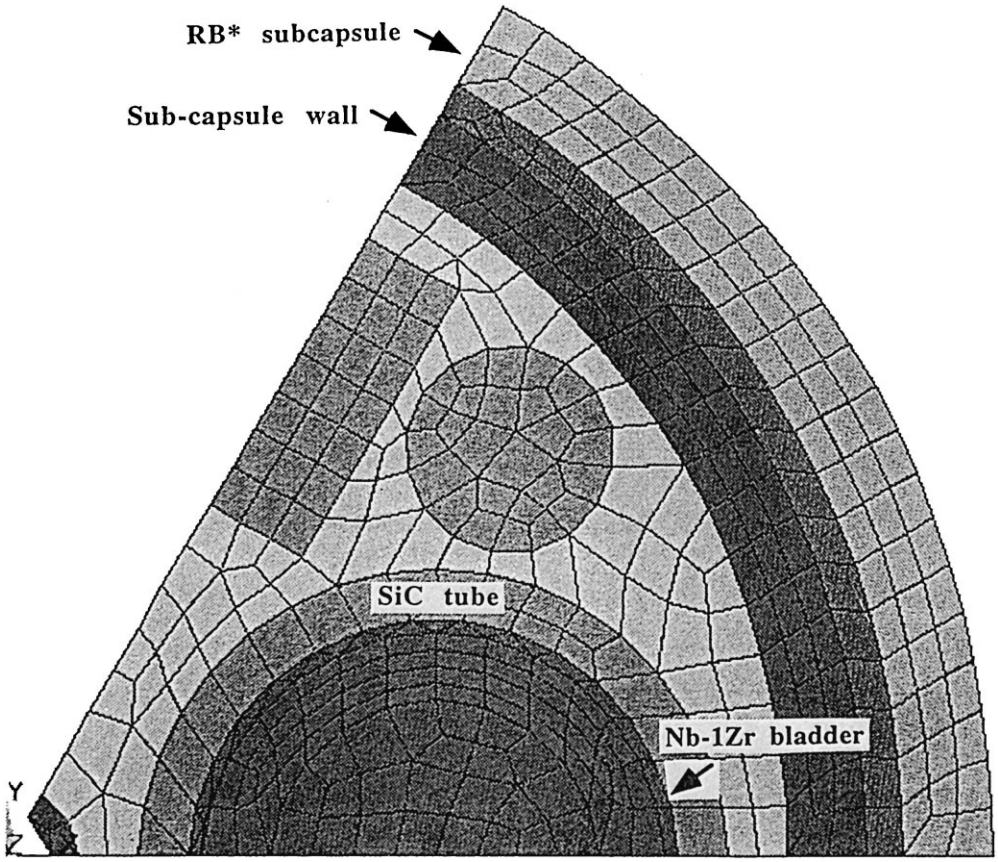

Fig. 7. FEM mesh used for 2D, sector model thermal analysis.

ence of the specimen is quite large, minor design modifications will mitigate this condition. Design changes such as using a thicker bladder tube (high thermal conductivity to even out temperatures) and making the fiber tube holder out of niobium–1 wt% zirconium (higher heating in a region where the temperature needs to be higher) would reduce this temperature gradient. Additional optimization studies are required to reduce the detrimental circumferential specimen temperature gradient. Nevertheless, extensive analysis during the design process indicates that, even with the potential for developing a temperature gradient across the samples, the pressurized bladder approach is the most suitable technique for investigating irradiation creep of SiC_f/SiC_m. Finally, it is recognized that there is uncertainty in the thermal analysis results. No attempt has been made to quantify the uncertainties, however it is expected the flexibility in the temperature control system is sufficient to compensate for these.

3.1.3. Chemical compatibility analysis

The experiment designed to measure the creep of SiC_f/SiC_m under irradiation involves using a niobium–1 wt% zirconium pressurized bladder in contact with a silicon carbide composite. Data regarding the compatibility between niobium–1 wt% zirconium and silicon carbide are not available. Therefore, the reactivity between niobium–1 wt% zirconium and silicon carbide was investigated by using a computer program (Chemsage) capable of calculating the Gibbs free energy of formation and rate of reaction for all compounds within the program database that can exist for a given thermodynamic state (pressure, temperature, number of moles). The actual reaction that will occur, however, will be limited by the kinetics of the transport mechanisms and the chemical reactions. A series of diffusion couple experiments was initiated to gather information on the kinetic aspects of the reactivity between niobium–1 wt% zirconium and silicon carbide.

Initially, the thermodynamic stability of niobium–1 wt% zirconium and β-silicon carbide (the phase present in the matrix of the chemical vapor infiltrated composites) was calculated at the lower end of the range of temperature of interest: 800°C, 1.01 bar total pressure, in pure helium. At this temperature, a niobium carbide (Nb_8C_7) and a silicide ($NbSi_2$) had a negative Gibbs free energy of formation, as did zirconium carbide (ZrC_4). This means that a reaction that produces these phases is energetically

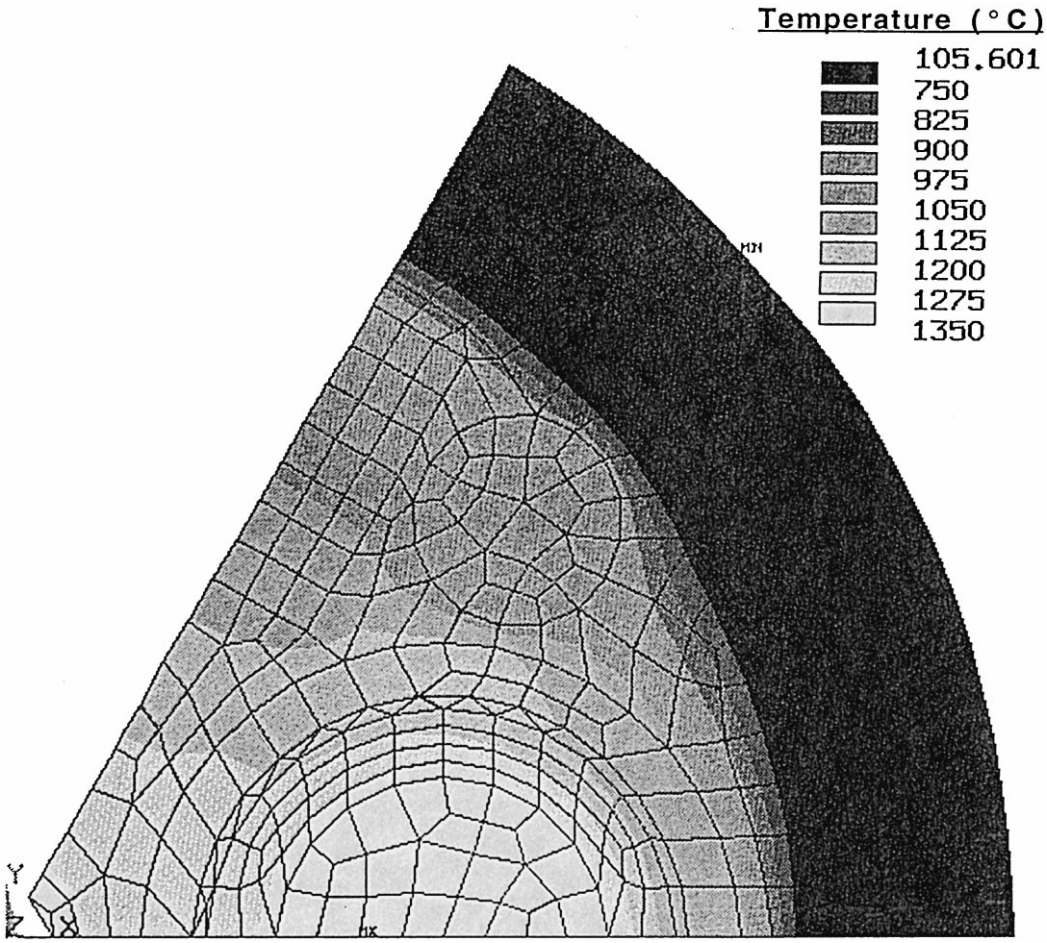

Fig. 8. Results of FEM 2D, sector model thermal analysis.

favorable. Furthermore, the thermodynamic calculations do not indicate metastable, or intermediate, phases that may also form.

The results of the initial thermodynamic calculation indicate that a diffusion-barrier coating must be placed between the niobium–1 wt% zirconium and the β-silicon carbide to prevent a detrimental reaction. Zirconia (ZrO_2), aluminum oxide (Al_2O_3) and a proprietary aluminide coating (aluminum oxide with minor amounts of chromium, iron and titanium) were selected as candidate coating materials. Based upon additional thermodynamic calculations, the most suitable coating material appears to be aluminum oxide (Al_2O_3).

Diffusion couple experiments were used to determine the kinetic stability of an aluminum oxide coating with niobium–1 wt% zirconium and β-silicon carbide. Diffusion couples consisting of a sandwich of niobium–1 wt% zirconium between two pieces of β-silicon carbide were used. The β-silicon carbide was fabricated by CVD, so that it would be similar to the matrix of the composite, and supplied by Morton Advanced Materials, Woburn, MA. One side of the niobium–1 wt% zirconium was coated with a 1 μm thick layer of alumina. The coating was deposited, at room temperature, by electron-beam sputter deposition, performed by Roger Johnson at PNNL. The clamping stress was designed to be of the order of 200 MPa, or slightly higher than the maximum stress anticipated in the creep experiment. The samples were heated for various times (100–400 h) in a resistively heated furnace, under flowing argon gas.

The diffusion couple specimens were examined via scanning electron microscopy (SEM), energy-dispersive X-ray spectroscopy (EDS), and Auger electron spectroscopy (AES). After the diffusion experiment, the alumina coating appeared much coarser in the scanning electron microscope. Despite appearing coarser, the width of the coating had not changed after the diffusion experiment. Mullite ($3Al_2O_3–2SiO_2$, or $2Al_2O_3–SiO_2$) may have

formed as a reaction product between the silicon carbide and alumina coating, or the alumina coating may have coarsened. Neither hypothesis has been investigated further.

A detailed investigation of the diffusion couple was performed with AES. Spot scans were conducted along a line crossing each interface at a distance of 4 μm apart. From this analysis a compositional profile was constructed (Fig. 9). The concentrations of each element are not absolute since the data has not been corrected for the various sensitivity coefficients. Nevertheless, the results indicate that there is very little interdiffusion on the side of the specimen with the coating. On the other hand, on the side without the coating some carbon and silicon may have diffused from the silicon carbide into the niobium–1 wt% zirconium and some niobium may have diffused into the silicon carbide. These results suggest that a diffusion-barrier coating can inhibit potential reactions between niobium–1 wt% zirconium and silicon carbide.

3.2. The in-pile tensile creep experiment

The previous sections describe approaches designed to measure the creep behavior of CVI SiC_f/SiC_m materials in reactor space available in the United States of America. The limitations of the available space preclude in situ tensile studies and a pressurized bladder method has been chosen as the most feasible technique for obtaining data. The pressurized bladder method, however, involves relatively complex experiments and is not a direct measurement of tensile creep strains. A parallel approach, intended to obtain creep strain data from tensile tests performed in a reactor, will be described below.

The proposed method would consist of loading flat, reduced gage-section specimens in tension, while in a reactor. The details of the specimen geometry will be determined from the space limitations of the reactor and the dimensions of the available SiC_f/SiC_m material. The proposed approach would utilize channel OK-70 in the reactor BR-10 in Obninsk, Russia. This channel has a diameter of 70 mm and a flux intensity nearing 7×10^{13} n/cm^2s. The working atmosphere is helium at 0.5–1.5 atm.

The specimens would be gripped in edge loading fixtures similar to those used by Holmes in high-temperature creep experiments on ceramic matrix composites [21]. The grips for each specimen would be machined from a solid piece of high-temperature, low activation material. The strain would be measured by monitoring the rotations of the load train driving motor. This method has been used extensively at the proposed facility and the reliability of the technique has been confirmed by post-test measurements and room temperature experiments outside the reactor using the same technique. The resolution of this technique varies with the creep rate of the material but it is typically 4–8 microns or a minimum creep rate of 10^{-7} h^{-1}. Although prior tests have been primarily torsion tests of thin walled cylinders, minimal modifications should be

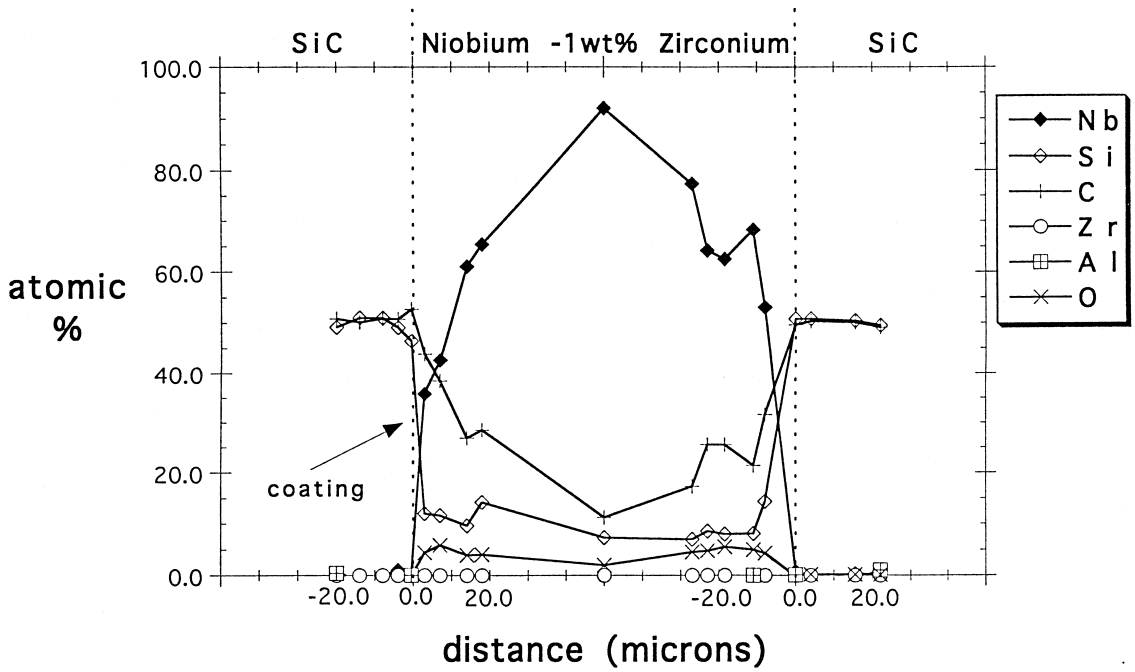

Fig. 9. Auger electron spectroscopy profile across diffusion couple specimens.

required to perform displacement controlled tensile tests. Currently, the maximum temperature from gamma heating in BR-10 is 600°C. Supplemental electric heating would be used to achieve higher temperatures. A detailed analysis of the in-pile tensile technique experiment is in progress.

4. Conclusions

A review of the available irradiation creep data suggests that the creep of silicon carbide is enhanced by irradiation. The use of SiC_f/SiC_m composites, therefore, in fusion energy systems necessitates study of their irradiation creep behavior. Two experimental techniques for obtaining irradiation creep data for SiC_f/SiC_m composites have been described. The stress state, temperature profile and chemical compatibility among assembly components for the pressurized bladder approach have been analyzed extensively. The analytical results indicate that the pressurized bladder approach is capable of demonstrating whether irradiation enhanced creep is of concern for the use of SiC_f/SiC_m in fusion energy systems. The in-pile tensile creep experiment is capable of providing real-time strain measurements, although the strain measurement resolution is lower than the pressurized bladder approach. Further analysis of the in-pile tensile specimen approach is in progress.

Acknowledgements

This work was also supported by the US Department of Energy (DOE) contract DE-AC06-76RLO 1830 with Pacific Northwest National Laboratory, which is operated for DOE by Battelle.

References

[1] R.H. Jones, C.H. Henager Jr., G.W. Hollenberg, J. Nucl. Mater. 191–194 (1992) 75.
[2] P. Fenici, H.W. Scholz, J. Nucl. Mater. 212–215 (1994) 60.
[3] H.W. Scholz, M. Zucchetti, K. Casteleyn, C. Adelhelm, J. Nucl. Mater. 212–215 (1994) 655.
[4] R.H. Jones, C.H. Henager Jr., J. Nucl. Mater. 212–215 (1994) 830.
[5] R.H. Jones, C.H. Henager Jr., J. Nucl. Mater. 219 (1995) 55.
[6] L.L. Snead, O.J. Schwarz, J. Nucl. Mater. 219 (1995) 3.
[7] R.J. Price, in: HTGR Base Program Quarterly Progress Report for the Period Ending August 31, General Atomic Division of General Dynamics Report GA-8200, 1967, p. 91.
[8] R.J. Price, Nucl. Technol. 35 (1977) 320.
[9] R. Scholz, A. Frias Rebelo, P. Dos Santos, Proc. of the IEA Workshop on Fusion Materials, Ispra, Italy, 1996.
[10] C.H. Carter Jr., R.F. Davis, J. Bentley, J. Am. Ceram. Soc. 67 (1984) 409.
[11] C.H. Carter Jr., R.F. Davis, J. Bentley, J. Am. Ceram. Soc. 67 (1984) 732.
[12] J.E. Lane, C.H. Carter, R.F. Davis, J. Am. Ceram. Soc. 71 (1988) 281.
[13] P.L. Farnsworth, R.L. Coble, J. Am. Ceram. Soc. 49 (1966) 264.
[14] P.M. Sargent, M.F. Ashby, Scr. Metall. 17 (1983) 951.
[15] D.F. Carroll, R.E. Tressler, J. Am. Ceram. Soc. 72 (1983) 49.
[16] G. Grathwohl, T.H. Reets, F. Thummler, Sci. Ceram. 11 (1981) 425.
[17] T.D. Gulden, C.F. Driscoll, Report No. GA-10366, Gulf General Atomic Co., 1971.
[18] X.J. Ning, P. Pirouz, J. Mater. Res. 6 (1991) 2234.
[19] X.J. Ning, P. Pirouz, S.C. Farmer, J. Am. Ceram. Soc. 76 (1993) 2033.
[20] C.A. Lewinsohn, C.E. Bakis, R.E. Tressler, Ceram. Trans. 38 (1993) 667.
[21] G.E. Hilmas, J.W. Holmes, R.T. Bhatt, J.A. DiCarlo, Ceram. Trans. 38 (1993) 291.